Article

Intensified Crystallization Processes for 1:1 Drug-Drug Co-crystals of Sulfathiazole-Theophylline, and Sulfathiazole-Sulfanilamide

Kuan Lin Yeh, and Tu Lee

Cryst. Growth Des., **Just Accepted Manuscript** • DOI: 10.1021/acs.cgd.7b01197 • Publication Date (Web): 16 Jan 2018

Intensified Crystallization Processes for 1:1 Drug-Drug Co-crystals of Sulfathiazole-Theophylline, and Sulfathiazole-Sulfanilamide

Kuan Lin Yeh and Tu Lee*

Department of Chemical and Materials Engineering, National Central University,

300 Zhongda Road, Zhongli District, Taoyuan City 32001, Taiwan R.O.C.

ABSTRACT

The chemical synthesis and crystallization step were integrated successfully for directly producing 1:1 co-crystal of sulfathiazole-theophylline and 1:1 co-crystal of sulfathiazole-sulfanilamide. The benefits of this process intensification were the reduction of number of steps, and the amount of energy consumption and solvent used. In addition, the overall co-crystal yields by Intensified Method I were much higher than the ones by Conventional Method. Intensified Method I also gave high-purity co-crystals of ≥ 99%. Sulfathiazole not forming co-crystals with sulfanilamide by

* Corresponding Author : Tel: +886-3-4227151 ext. 34204. Fax: +886-3-4252296, Email: tulee@cc.ncu.edu.tw

Intensified Method I, was dissolved in the mother liquor by taking advantage of the pH-dependent solubility of sulfathiazole. Co-crystals of both sulfathiazole-theophylline and sulfathiazole-sulfanilamide systems remained stable under conditions of 40 ^{o}C and 75% relative humidity for a month.

INTRODUCTION

Co-crystal is defined as a crystalline solid composed of two or more distinct compounds in a definite stoichiometric ratio. Those distinct components are originally in solid state under ambient conditions. The crystalline framework of co-crystal is held together by non-covalent interactions such as van der Waals forces, halogen bonding, π-π stacking, and especially hydrogen bonding.[1] Unlike salts, pharmaceutically acceptable co-crystals are not merely restricted to active pharmaceutical ingredients (APIs) with an ionizable site. A wide range of co-crystal formers (i.e. co-formers according to the list of generally recognized as safe (GRAS)) offers more flexibility for tailoring the physiochemical properties of APIs such as melting point,[2] solubility,[3] dissolution rate,[4] bioavailability,[5] compressibility[6] and moisture stability[7] without changing the effective chemical entity of APIs. Since about 70 % of new drug candidates and many commercial drugs suffer from inadequate physicochemical properties such as solubility, dissolution rate and

bioavailability,[8] co-crystallization has attracted more and more attention, and become an important tool in pharmaceutical product design. [4,9,10]

However, from a process design point of view, process intensification is a concept of transforming a conventional chemical process into a more economical, productive and greener process.[11] In the past decades, the same concept has evolved into a paradigm for better process performance and higher product quality, and more lucrative and safer technologies through the improvement of manufacturing process. The utilization of new apparatus and technique as an alternative can reduce processing times, solvent and energy consumption, number of processing steps and equipment size.[11,12] In general, APIs and fine chemicals are firstly made by chemical synthesis, and then isolated and purified by crystallization.[13,14] And yet, for most of the studies, only co-crystallization between API and co-former was investigated without giving consideration to chemical synthesis and co-crystallization as a whole. Therefore, our past success in integrating the synthesis of API and co-crystallization by the approach of direct co-crystal assembly[15] has prompted us to look into more complicated co-crystal systems, and finally implement process intensification method.

Sulfathiazole (STZ) and sulfanilamide (SNM) were chosen as two model sulfa drugs in our present study. Both drugs possessed a sulfonamide group, and were used as antibacterial APIs through the history of human.[16] Although sulfa drugs had

already been replaced by antibiotics due to the drug-resistant strains, sulfa drugs are still being investigated extensively because of their low cost, excellent activity and popularity.[17,18] Several co-crystal systems of STZ and SNM had been discovered and reported in the literature.[19-21] They included 1:1 co-crystal of STZ-glutaric acid, 1:1 co-crystal of STZ-4-aminobenzamide, 1:1 co-crystal of sulfathiazole-theophylline (STZ-THE) and 1:1 co-crystal of STZ-SNM, which were prepared by grinding and evaporation on a small scale. Among those co-crystal systems, 1:1 co-crystal of STZ-THE and STZ-SNM, were chosen as the two drug-drug co-crystals produced by the intensified crystallization processes in our present study. Interestingly, STZ and SNM can be synthesized from the same chemical reaction, and THE is a commonly used API in pharmaceutical co-crystals.[22]

The drug-drug co-crystal system is a co-crystal made up of two APIs.[23] The drug combo has been an approach to offer a synergistic therapy in recent years.[24] It shows potential advantages of reducing drug dosage, toxicity and resistance, and enhancing the efficacy of therapy.[25-27] Since the drug-drug co-crystals have a higher degree of unpredictability than the one of drug combos and ordinary type of co-crystals, they are more patent eligible. As a consequence, there is a strong incentive to design drug-drug co-crystals. For example, valsartan-sacubitril·3Na·2.5H_2O having a brand name of Entresto®,[28] is a commercial

product comprising of co-crystals of valsartan salt and sacubitril salt. Entresto® has shown a better effect on treating heart failure than the other traditional medicines.[29] It is also a demonstration of using co-crystal to prolong the life-cycle management of an API.

Since the development of intensified processes requires the integration of chemical synthesis and co-crystallization of STZ and SNM, the understanding of each synthetic and co-crystallizing step, and product analysis becomes essential. Therefore, the aims in our study include the determination of: percent yield and purity given by different processes, pH-dependent solubility, partition coefficient (log P) and moisture stability of co-crystals. The percent yield and purity for the co-crystals of STZ-THE, and STZ-SNM, obtained by conventional methods and intensified processes have been compared for evaluating the feasibility of process intensification. It was reported that sulfonamide-induced crystalluria (i.e. sulfa drugs) in urinary tract is highly dependent on the solubility and concentration of the sulfa drugs in urine in the pH range of 5.5 to 7.0.[30,31] Therefore, the effect of pH on solubility for the co-crystals has been studied. In addition, the values of solubility, log P, moisture stability for co-crystals have also been determined.

MATERIALS AND METHODS

Materials. 2-Aminothiazole ($C_3H_4N_2S$; 97 % purity; MW, 100.14; Lot: 10163024) was purchased from Alfa Aesar (Heysham, England). *N*-acetylsulfanilyl chloride ($C_8H_8ClNO_3S$; 98% assay; MW, 233.67; Lot: STBD9067V) and theophylline ($C_7H_8N_4O_2$; ≥99% purity; MW, 180.16; Lot: SLBF2355V) were purchased from Sigma-Aldrich (China). 1-octanol ($C_8H_{18}O$; 97% assay; M.W. 130.2; Lot: E39586), ammonium hydroxide (NH_4OH; 28-30% assay; MW, 35.05; Lot: E51053), sodium bicarbonate ($NaHCO_3$; 99.7-100.3% assay; MW, 84.01; Batch No: 0000085775) and sodium chloride (NaCl, ≥ 99% assay; MW, 58.44; Batch No: 0000031282) were purchased from J. T. Baker (USA). Sulfanilamide ($C_6H_8N_2O_2S$; MW, 172.20; Batch No: 0000099327) was purchased from J. T. Baker (China). Sodium hydroxide (NaOH; 96% assay; MW, 40.00; Lot: KX-2842A) was purchased from Showa Chemical Co., Ltd. (Tokyo, Japan). Sulfathiazole ($C_9H_9N_3O_2S_2$; ≥ 98% assay; MW, 255.32; Lot: 410504) was purchased from Fluka (Steinheim, USA). Acetone (CH_3COCH_3; 99.5% purity; MW, 58.0; Lot: EB8n311) and methanol (CH_3OH; 99.9% assay; MW, 32.04; Lot: 14050368) were purchased from Tedia Company Inc. (Fairfield, OH, USA). Hydrochloric acid (HCl; 37% assay; MW, 36.46; Lot: UN1789) was purchased from Scharlau Chemie S.A. (Barcelona, Spain). Reversible osmosis (RO) water was clarified by a water purification system (model Milli-RO Plus) bought from Millipore (Billerica, MA, USA). All of the chemicals were used

without further purification.

Instruments. Optical Microscopy (OM). Crystal habit was observed by optical microscopy (Olympus BX-51, Tokyo, Japan) equipped with a digital camera (Moticam 2000)) and a cross polarized filter. The micrograph was transformed through Motic Images Plus (Version 2.0) into a digital photograph and analyzed by Measure Tool (Version 4.10).

Thermogravimetric Analysis (TGA). TGA analysis was carried out by TGA 7 (Perking Elmer, Norwalk, CT) to monitor sample weight loss as a function of temperature. All samples were heated under nitrogen atmosphere to avoid oxidation. About 3-6 mg of samples were weighed and placed on an open platinum pan suspended in a heating furnace. The heating rate was 10 $^{o}C \cdot min^{-1}$ and the temperature range of scan was from 40 ^{o}C to 280 ^{o}C.

Differential Scanning Calorimetry (DSC). Thermal analytical data were obtained by Perkin Elmer DSC-7 calorimeter (Shelton, CT, USA). Each sample was loaded in a perforated aluminum pan, and characterized with a scanning rate of 10 $^{o}C \cdot min^{-1}$ from 40 ^{o}C to 240 ^{o}C under a constant 99.99% nitrogen purge.

Fourier-Transform Infrared (FT-IR) Spectroscopy. FT-IR spectroscopy was conducted on Perkin Elmer Spectrum One (Norwalk, CT, USA.) to identify functional groups and polymorphs. Each sample was ground gently with potassium bromide

(KBr) powders in a ratio of 1 to 100 and then a hydraulic press was used to form a tablet. The tablet was scanned 8 times with a resolution of 2 cm^{-1} in the wavenumber region of 4000 to 400 cm^{-1}.

Powder X-ray Diffraction (PXRD). PXRD diffractograms were conducted by Bruker D8 Advanced (Germany), whose source used was Cu Kα (λ = 1.542 Å), and the diffractometer was operated at 40 kV and 40 mA. The X-ray passed through a nickel filter with a divergence slit of 0.5°, a scattering slit of 0.5°, and a receiving slit of 1 mm. The scanning rate was set at 0.05° 2θ·sec^{-1} ranging from 2θ = 5° to 35°.

Nuclear Magnetic Resonance (NMR). About 40 mg of dried sample powders were dissolved in an adequate amount of deuterated dimethyl sulfoxide (DMSO-d_6). Around 0.8 mL of the sample solution was added into an NMR tube having a 5-mm in outer diameter and 178 mm in length for solution ^{1}H-NMR analysis (Bruker Ascend^{TM} 600 MHz). Chemical shifts were relative to the one of DMSO at 2.50 ppm. Resonance peak areas were integrated by MestReNova (Version 11.0.4) software from Mestrelab Research S. L.

Ultraviolet and Visible (UV/vis) Spectrophotometer. UV/Vis spectrophotometer (Lambda 25, Perkin Elmer, Norwalk, CT, USA) was used to measure the concentrations of STZ, SNM, STZ-THE and STZ-SNM at the characteristic absorption peaks of 283, 258, 277 and 258 nm, respectively. The concentrations of

STZ, SNM, STZ-THE, and STZ-SNM were converted from the absorbance values to the corresponding concentrations by the linear calibrations of: absorbance (au) = 49666 × concentration of STZ (M), absorbance (au) =15650 × concentration of SNM (M), absorbance (au) =27728 × concentration of STZ-THE (M), absorbance (au) =31807 × concentration of STZ-SNM (M), respectively, as determined in water at 25 ^{o}C.

High-Performance Liquid Chromatography (HPLC). HPLC analysis was performed using a Shimadzu Prominence-i LC-2030C 3D HPLC. Sample solutions were prepared by dissolving 5 mg of sample powders in 25 mL of methanol. 2 μL of sample was withdrawn and injected into a column (YMC-Pack ODS-AQ 150×3.0 mm×3 μm×12nm). The mobile phase used was a gradient system composed of methanol/0.05 % formic acid aqueous solution. The composition of the mobile phase started at 5/95 (v/v), increased to 90/10 (v/v) in 15 min, and maintained for 5 min. The flow rate was 0.5 mL·min^{-1} and the temperature was kept at 37 ^{o}C. The detection wavelength for HPLC was set at λ = 254 nm.

Experiments.

Syntheses of STZ and SNM. For the synthetic processes of STZ and SNM, each process was divided into two steps. In Step 1 (Scheme 1): 6 g (25.7 mmol) of

N-acetylsulfanilyl chloride were slowly added to the suspension containing 1.25 g (12.5 mmol) of 2-aminothiazole, 2.25 g (26.8 mmol) of sodium bicarbonate and 3 g (51.3 mmol) of sodium chloride in 11 mL of water and 5.5 mL of acetone in a 100 mL round-bottom flask at 25 ^{o}C to 30 ^{o}C under agitation for 2.5 h. *N*-acetylsulfanilyl chloride was fed as six equal portions for avoiding the fast evolution of CO_2 which was a by-product of neutralization between HCl and $NaHCO_3$. 3.1 mL of 28~30 wt% NH_4OH solution were added to the reaction mixture. Afterwards, the resulting mixture was heated to 65 ^{o}C with a total reflux for 2.5 h. After the reaction solution was cooled to room temperature, N^4-acetyl SNM was precipitated, filtered and rinsed by 15 mL of cold water twice. The mother liquor was treated with 0.25 g of Darco for decolorization. It was then stirred for 1 h, and filtered for the removal of Darco particles. The pH of filtrate was adjusted to 5 to 6 by adding 12~14 mL of 2M HCl aqueous solution to precipitate out N^4-acetyl STZ. N^4-acetyl STZ solids were filtered and rinsed with cold water twice. Solids of N^4-acetyl SNM and N^4-acetyl STZ were oven dried at 40 ^{o}C overnight.

In Step 2a (Scheme 1): 2.97 g (10 mmol) of N^4-acetyl STZ solids were added into a 50 mL round-bottom flask with a magnetic spin bar. 12.5 mL of 3.2 M NaOH aqueous solution were then introduced into the flask for hydrolysis, and the reaction solution was heated to 65 ^{o}C in a water bath for 2 h. The reaction solution was then

acidified by adding 15 mL of 2 M HCl aqueous solution to produce STZ solids. On the other hand, 1.07 g (5 mmol) of N^4-acetyl SNM solids were reacted with 10 mL of 1.5 M HCl aqueous solution for hydrolysis in a 25 mL round-bottom flask, and heated to 95 to 100 ^{o}C in an oil bath with a reflux for 4 h. Then, the reaction solution was cooled to 20 ^{o}C, treated with 25 mg of Darco and stirred for 30 min, and then filtered for the removal of Darco. The mother liquor was neutralized by adding 4M NaOH aqueous solution to adjust the pH to 4~5 to precipitate SNM solids. All harvested solids were filtered, rinsed with copious amounts of cold water twice and oven dried at 40 ^{o}C overnight.

Cooling Co-crystallization of STZ-THE. Synthesized STZ crystals were replaced by the use of purchased STZ crystals for the control experiment. 1 g of purchased THE was totally dissolved in 160 mL of methanol in a 0.5 L flat-bottom flask with an inner diameter of 7.4 cm equipped with four equally spaced vertical baffles, a four bladed turbine impeller made of stainless steel, and a total reflux condenser. The temperature was maintained at 60 ^{o}C. An equimolar amount of purchased STZ crystals was dissolved in 60 mL of methanol, and added into the flask, and mix with the solution of THE. The co-crystallization was carried out by cooling the solution from 60 ^{o}C to 20 ^{o}C at a stirring rate of 600 rpm.

Cooling Co-crystallization of STZ-SNM. Synthesized SNM crystals were replaced

by the use of purchased SNM crystals for the control experiment. 1.29 g of purchased SNM and 1.53 g of purchased STZ were added together in a 100 mL scintillation vial. 60 mL of preheated methanol were introduced into the vial to simultaneously dissolve SNM and STZ at 60 ^{o}C using a magnetic spin bar. Then, the solution was cooled to 20 ^{o}C to form 1:1 co-crystal of STZ-SNM.

Intensified Method I. For direct preparation of 1:1 co-crystal of STZ-THE, 5 mL of 4 M HCl aqueous solution were added right after hydrolysis. An equimolar amount of purchased THE with respect to N^4-acetyl STZ, and 3.5 mL of 4 M HCl aqueous solution were added to the reaction solution to produce 1:1 co-crystal of STZ-THE. For direct preparation of 1:1 co-crystal of STZ-SNM, an equimolar amount of purchased STZ with respect to N^4-acetyl SNM was introduced immediately after hydrolysis. The solution was treated with 25 mg of Darco, stirred for 30 min, and then filtered for the removal of Darco particles. *The pH value of the resulting solution was adjusted to 9 for producing the 1:1 co-crystal of STZ-SNM.* All solids harvested were filtered, rinsed with cold water twice, and then dried at 40 ^{o}C overnight.

Intensified Method II. 2.14 g (10 mmol) of N^4-acetyl SNM and 20 mL of 1.5 M HCl aqueous solution were added into a 25 mL round-bottom flask. The reaction solution was heated to 95 to 100 ^{o}C in an oil bath equipped with a reflux condenser

for 4h to give a SNM-containing solution. Afterwards, the SNM-containing solution was cooled to room temperature for the ease of operation, treated with 25 mg of Darco, stirred for 30 min, and then filtered for the removal of Darco. Additionally, 2.97 g (10 mmol) of N^4-acetyl STZ and 20 mL of 3.2 M NaOH aqueous solution were added together into a 50 mL round-bottom flask. The solution was heated to 65 ^{o}C for 2 h to give a STZ-containing solution. 1:1 co-crystal of STZ-SNM was precipitated out by introducing the SNM-containing solution into the STZ-containing solution at 65 ^{o}C. All solids were filtered, rinsed with cold water twice, and oven dried at 40 ^{o}C overnight.

Solubility Test. Solubility test was performed at 15 ^{o}C, 25 ^{o}C, 40 ^{o}C and 60 ^{o}C in water. Each unsieved solid sample was weighed into a 20 mL scintillation vial. Water was titrated dropwise in a vial at a fixed temperature in a water bath. The solution was shaken intermittently by hand. Water was gradually added within 6 hours until all solids were just dissolved as determined by eyes. This titration method was simple and robust, provided solubility values, and minimized the possibility of solvate and hydrate formation during the measurements. The total volume of water added was recorded and the solubility was also calculated in terms of molarity (M).[32]

pH Dependence in Solubility. Each solid sample was weighed and suspended in

water in a 100 mL scintillation vial. The pH value of each suspension was adjusted by adding HCl and NaOH aqueous solutions. The suspension was kept at 37 ^{o}C for a day to achieve equilibrium, and then filtered through a 0.22 μm PVDF membrane (PALL Corporation, PN). The mother liquors were assayed by a UV/vis spectrophotometer, and the solids were characterized by DSC.

Partition Coefficient Determination. Around 2-3 mg of sample powders were weighed into a 100 mL scintillation vial comprising of 15 mL of water with an equal volume of 1-octanol at 25 ^{o}C. The solutions were shaken for 40 h. Afterwards, only the aqueous phase was assayed by HPLC.

Moisture Stability Test. Each solid sample was weighed into a 7 mL open vial, which was placed in a capped 100 mL glass bottle filled with 10 mL of saturated NaCl aqueous solution to have a closed system at 40 ^{o}C and 75% relative humidity (RH) for a month.[7] The sample was then characterized by DSC.

RESULTS AND DISCUSSION

Syntheses of STZ and SNM

There were five polymorphs for STZ (Forms I to V), and four modifications for SNM (Forms α to δ).[33-35] According to the literature, Form III is the most stable form for STZ, and Form β is the most stable form for SNM under the ambient

condition.[36,37] The transition temperature of STZ from Form III is reported at 175 °C followed by a melting point of Form I at 202 °C.[36,38] Form β had a phase transition to Form γ at 131 °C to 141 °C before melting at 166 °C.[39] For the integration of chemical synthesis and co-crystallization, a good understanding of process and crystal forms was necessary. Therefore, STZ and SNM were synthesized and analyzed as controls. The preparation processes of STZ, SNM, 1:1 co-crystal of STZ-THE and 1:1 co-crystal of STZ-SNM were shown in Scheme 1. Step 2 in Scheme 1 was categorized into three methods: Conventional Method, Intensified Method I and Intensified Method II.[40,41] As indicated by Step 2a, STZ and SNM were obtained via hydrolyzing N^4-acetyl STZ by the base addition, and N^4-acetyl SNM by the acid addition, respectively. They were both crystallized out by neutralization. In addition to the reaction-related factors such as percent yield and purity, polymorphism of API solids is equally important, and needs to be controlled due to its profound effect on the quality of a final product.

The IR assignments for Form III STZ crystals were shown in Figure 1. The bands at 3279 cm^{-1} and 3320 cm^{-1} were assigned for the $–NH_2$ symmetric and asymmetric stretching vibrations, respectively. The $–SO_2–$ symmetric and asymmetric stretching vibration frequencies are found at 1136 cm^{-1} and 1323 cm^{-1}, respectively. The bands at 1531 cm^{-1} can be contributed to C=N stretching vibration,

and 631 cm^{-1} to C–S stretching frequency.[19,42] The FT-IR spectrum of synthesized STZ in Figure 1(b) matched well with the one of purchased STZ crystals in Figure 1(a), indicating that the synthesized STZ crystals were chemically identical to the purchased STZ crystals, which were Form III STZ crystals.[43] The band assignments for Form β SNM crystals were as follows: 3477 cm^{-1} and 3370 cm^{-1} for $–NH_2$ symmetric and asymmetric stretching vibrations, respectively, 1313 cm^{-1} and 1146 cm^{-1} for $–SO_2–$ symmetric and asymmetric stretching vibrations, respectively, and 900 cm^{-1} for S–N stretching vibration.[42,44] Synthesized SNM in Figure 1(d) gave a different IR spectrum from the one of purchased SNM crystals in Figure 1(c). The characteristic bands at 3375 cm^{-1} and 3266 cm^{-1}, and the ones at 3383 cm^{-1}, 3318 cm^{-1} and 3243 cm^{-1} were corresponding to Form β and Form γ SNM crystals, respectively.[39] The absorption region of 3235 cm^{-1} to 3380 cm^{-1} was used to distinguish Form γ crystals from the other polymorphs of SNM crystals. The synthesized SNM crystals are not always the most stable Form β. Although the purchased SNM crystals and synthesized SNM crystals possess an identical molecule, the packing arrangements of molecules are different.

There was a good agreement among the PXRD patterns of purchased and synthesized STZ crystals in Figures 2(a) and 2(b), respectively, and the theoretical pattern of Form III STZ crystals based on single-crystal X-ray experiment in Figure

2(c). This was also evidenced by the IR spectra in Figures 1(a) and (b). The slightly shifted diffraction peaks for synthesized STZ crystals in Figure 2(b) were most likely attributed to the build-in strain of crystal originated from the lengthening or shortening of the d-spacing[45] when the synthesized STZ crystals were precipitated out rapidly by the addition of HCl aqueous solution into the reactor. The diffraction pattern of purchased SNM in Figure 3(a) was consistent with the theoretical one of Form β SNM crystals in Figure 3(c). The PXRD diffractogram of synthesized SNM crystals in Figure 3(b) matched with the theoretical one of Form γ SNM crystals in Figure 3(d). However, several additional peaks at $2\theta = 18.97^{o}$, 20.61^{o}, 21.45^{o} and 22.85^{o} designated for Form β SNM crystals were also detected for the synthesized SNM crystals in Figure 3(b), meaning that the synthesized SNM crystals were adulterated with a trace amount of Form β SNM crystals.

According to the Ostwald's Rule of Stages,[46] the metastable synthesized Form γ SNM crystals would eventually transform to the most stable Form β SNM crystals if given with a long enough residence time in the reactor or a stimulus from downstream processes and storage. Drug properties will be altered when API is transformed into a different polymorph. Since the presence of different polymorphs in a final product is deemed as contamination, this kind of uncontrolled situation should be avoided.[47] Controlling the polymorphism of synthesized SNM crystals may be challenging in a

scale-up process because of the local variations in concentration and temperature. This gave us the motivation to employ Intensified Method to turn the polymorphic SNM solids into isomorphic co-crystals directly during synthesis to avoid polymorphic impurity.

Cooling Co-crystallization of STZ-THE and STZ-SNM.

The discovery of 1:1 co-crystal of STZ-THE and 1:1 co-crystal of STZ-SNM were first reported in 1971.[20] However, the physicochemical data about those two co-crystal systems such as melting point, crystal habit, solubility and stability were unavailable. Due to the lack of physicochemical data in the literature, STZ-THE co-crystals and STZ-SNM co-crystals were prepared in methanol by cooling co-crystallization as control. Synthesized STZ and SNM crystals were replaced by the use of purchased STZ and SNM crystals in Conventional Method for the controlled experiments. The two co-crystals produced by cooling were abbreviated as Cocry-STZ-THE and Cocry-STZ-SNM. The weight losses of Cocry-STZ-THE and Cocry-STZ-SNM co-crystals started at about 230 ^{o}C due to chemical degradation (Figure S1). Therefore, the temperature scanning range for DSC was set from 40 ^{o}C to 240 ^{o}C. Other data for Cocry-STZ-THE and Cocry-STZ-SNM co-crystals would be discussed in detail along with the ones for the co-crystals produced by Intensified

Method I in the next section.

Preparation of STZ-THE and STZ-SNM and by Intensified Method I

The 1:1 co-crystal of STZ-THE and 1:1 co-crystal of STZ-SNM produced by the Intensified Method I were abbreviated as Inten-I-STZ-THE and Inten-I-STZ-SNM co-crystals, respectively, in Scheme 1, Step 2b. The purchased THE and STZ crystals were fed to the reaction solution consisting of STZ and SNM species after hydrolysis, respectively, and formed STZ-THE and STZ-SNM co-crystals after neutralization. The products were changed from the original APIs to the co-crystals. Figures 4 and 5 showed the PXRD patterns of STZ-THE and STZ-SNM co-crystals obtained from *cooling co-crystallization* (i.e. *Conventional Method*) and Intensified Method I, and their theoretical patterns based on single-crystal X-ray crystallography.[20] They matched well with each other. The relative intensity of the diffraction peaks in Figures 4 and 5 varied from method to method. We speculated that this was caused by the solvent effect on growth rate of different crystallographic direction.[48]

Cocry-STZ-THE and Cocry-STZ-SNM co-crystals exhibited the endotherms of melting at 227.7 ^{o}C and 182.3 ^{o}C in Figures 6 (b) and 6(d), respectively. The co-crystals produced by Intensified Method I showed the same endothermic peak in Figures 6(b) and 6(d). Both DSC and PXRD results indicated that STZ-THE and

STZ-SNM co-crystals were successfully prepared by Intensified Method I using a one-pot process. Moreover, no detectable trace of SNM polymorph was present in the DSC scans for Inten-I-STZ-SNM co-crystals. The possibility of forming different SNM polymorphs was minimized by forming co-crystals using Intensified Method I. Crystallinity for all solids was determined by DSC based on Equation (1):[49]

$$Crystallinity\,(\%) = (\Delta H_{sp}^{f} / \Delta H_{pp}^{f}) \times 100\% \quad (1)$$

where ΔH_{sp}^{f} = enthalpy of fusion for samples, and ΔH_{pp}^{f} = enthalpy of fusion for a standard. Cocry-STZ-THE and Cocry-STZ-SNM co-crystals were defined as the calculation standards. STZ and SNM crystals can be dissolved in either a strong basic or acidic aqueous solution, and then precipitated out by neutralization.[40] STZ crystals were precipitated out from the basic mother liquor instantly upon the addition of HCl aqueous solution, indicating of a relatively high degree of supersaturation due to the drastic decrease of solubility. In general, a high degree of supersaturation gives solids with a low degree of crystallinity.[50] The enthalpies of fusion for both Inten-I-STZ-THE and Inten-I-STZ-SNM co-crystals were close to the ones for Cocry-STZ-THE and Cocry-STZ-SNM co-crystals, meaning that the co-crystals produced by Intensified Method I have a high degree of crystallinity. FT-IR spectra

of STZ-THE and STZ-SNM co-crystals were shown in Figures S2 and S3 of Supporting Information, respectively. The spectra of co-crystals generated by Intensified Method matched well with the ones by cooling co-crystallization in Conventional Method.

Various loading ratios (LRs) of N^4-acetyl STZ to THE, and N^4-acetyl SNM to STZ were attempted to further investigate the effect of addition amount of co-former. The melting point of Inten-I-STZ-THE co-crystals in Figure S4a could vary while the LR of N^4-acetyl STZ to THE, was changed from 1:1.4 to 1:0.6. Noticeably, a new endothermic peak appeared at 167.3 ^{o}C (Figure S4a(i)) as the LR was lowered to 1:0.6. We speculated that the original endothermic peak of 175 °C for Form III STZ crystals might be depressed to a lower temperature of 167.3 ^{o}C due to the presence of STZ-THE co-crystals. In addition, a new endothermic peak of 157.7 ^{o}C was observed for the sample with the LR of 1:0.5 (Figure S4b(i)), whereas another new endothermic peak of 165.8 ^{o}C was seen in the DSC scan for the sample having the LR of N^4-acetyl SNM to STZ of 1:1.5 (Figure S4b(iii)). The appearance of the two endothermic peaks in Figures S4b(i) and S4b(iii) was ascribed to the excess amount of SNM and STZ crystals, respectively. However, the original melting points of Form γ SNM crystals and Form III STZ crystals are 166 ^{o}C and 175 ^{o}C, respectively.[36,39] A possible explanation for the shift of the endothermic peaks was

due to eutectic behavior of mixing of SNM crystals with STZ-SNM co-crystals, and STZ crystals with STZ-SNM co-crystals. This kind of eutectic behavior leads to the depression of melting point, which had been reported in other co-crystal systems.[51-53] This was further evidenced by performing the DSC scans on the physical blend of purchased SNM crystals and Cocry-STZ-SNM co-crystals with a molar ratio of 1:1, and the physical blend of purchased STZ crystals and Cocry-STZ-SNM co-crystals with a molar ratio of 1:1, as displayed in Figure S5. It seems that the LR of 1:1 is the best ratio to produce the pure co-crystals of STZ-THE, and STZ-SNM.

Agreeing with the DSC scan in Figure S4, when the LR was varied, one of the co-crystal components was present as an isolated component in the co-crystal product. A solid mixture was produced once the LR was deviated from 1:1 significantly. For example, the characteristic diffraction peaks of THE crystals were detected when the LR was increased to 1:1.2, and 1:1.4 in the Inten-I-STZ-THE system (Figure S6(d) and (e)). As for the Inten-I-STZ-SNM in Figure S7, the PXRD pattern of STZ-SNM system with the LR of 1:1.5 in Figure S7(c) consisted of the diffraction peaks of STZ-SNM co-crystals and a trace amount of Form III STZ crystals, and yet, the diffraction peaks of pure SNM were absent for the system using LR of 1:0.5 in Figure S7(a). The trace level of SNM crystals might be below the detection limit of PXRD, which had been used to quantify the amount of co-crystals in a mixture with the limit

of 1.23 wt%.[54] Besides, we had tested the PXRD detection limit by powder blends having different weight percentages of purchased SNM crystals to Cocry-STZ-SNM co-crystals of 4 wt%, 5 wt% and 10 wt%. The diffraction peak at $2\theta = 10.6^{o}$ representing SNM crystals was found for the powder blends containing 5 wt% and 10 wt% SNM crystals, and disappeared for powder blends having 4 wt% SNM crystals as shown in Figure S8. Therefore, only 4 wt% or less of SNM crystals were present if there was any in the product of Inten-I-STZ-SNM co-crystals using LR of 1:0.5.

The ^{1}H NMR spectra in Figure S9 showed that all resonance peaks could be assigned to the specific protons of STZ or THE molecules, and STZ or SNM molecules,[55] for Inten-I-STZ-THE, and Inten-I-STZ-SNM co-crystals, respectively. No by-product was generated upon the formation of co-crystals in Intensified Method I.

Figure 7 displayed the crystal morphology for STZ and SNM crystals, and STZ-THE and STZ-SNM co-crystals. The synthesized STZ, and SNM crystals had rhombic, and thin plate-like habits, respectively. The STZ-THE co-crystals also exhibited a rhombic morphology regardless of the method used. The rhombic morphology of the STZ-THE co-crystals (Figure 7(c) and S7(d)) was more regular than the one of synthesized STZ crystals. In general, a more regular shape can lead to better manufacturability such as flowability, which can benefit downstream

processes including blending, granulation and tableting.[56] However, Cocry-STZ-SNM and Inten-I-STZ-SNM co-crystals had a rod-like habit, which was unfavorable for the downstream processes. The rod-like or needle-like crystals generally leads to a low power flow, poor compressibility and high filtration resistance.[56,57]

According to Scheme 1, Conventional Method was comprised of the steps of reaction, crystallization of API, two sets of filtration and drying, addition of co-former and co-crystallization. For Intensified Method I, crystallization of API, and a set of filtration and drying can be omitted. Generally speaking, the number of processing steps is directly proportional to time, energy, waste and labor intensity. In this regard, Intensified Method I is more advantageous over Conventional Method. Table 1 revealed the percent yields of synthesized STZ crystals, synthesized SNM crystals, Cocry-STZ-THE, Cocry-STZ-SNM, and Inten-I-STZ-THE and Inten-I-STZ-SNM co-crystals produced with LR of 1:1. We found that the co-crystal yield of 81.0% for STZ-THE solids by Intensified Method I was higher than the one of 68.1% by cooling co-crystallization. On the other hand, the co-crystal yields for STZ-SNM by Intensified Method I and the cooling co-crystallization were almost the same. Remarkably, the overall co-crystal yields by Intensified Method I were much higher than the ones by Conventional Method when including the synthetic steps. In

addition, when the feeding rate of the HCl aqueous solution was too fast, fine STZ crystals were produced and tended to agglomerate into large lumps. However, if THE crystals were introduced prior to neutralization, no agglomerates were formed even with the same fast addition rate of HCl aqueous solution.

HPLC data were provided in Figure S10 and the results were tabularized in Table 2. The retention times of STZ, SNM and THE molecules were 6.4, 3.4 and 7.2 min, respectively. According to the HPLC results, Intensified Method I gave all harvested samples a purity of ≥ 99%. The stoichiometric ratios of STZ to THE, and STZ to SNM crystals were calculated based on the ratios of the integration peak areas of the dissolved STZ to THE species, and the dissolved STZ to SNM species, respectively. All ratios were very close to one. The results indicated that the 1:1 co-crystals produced had a very high purity.

Preparation of STZ-SNM by Intensified Method II

According to Scheme 1, Step 2b, the reaction solutions of STZ, and SNM were basic and acidic, respectively, and their crystallizations were carried out through neutralization, by adding HCl, and NaOH aqueous solution, respectively. Since the solids were co-crystallized through neutralization in Intensified Method I which gave us the idea that those two processes could be further combined to prepare STZ-SNM co-crystals. Therefore, the two reaction solutions of N^4-acetyl STZ and N^4-acetyl

SNM after hydrolysis were mixed together to yield STZ-SNM co-crystals (Scheme 1, Step 2c). This approach was called Intensified Method II. STZ and SNM species were present separately in the aqueous solutions before mixing for co-crystallization. The solution phase was more convenient for feeding and mixing than the powder form.

Although the PXRD pattern of Inten-II-STZ-SNM co-crystals matched with the theoretical pattern of STZ-SNM co-crystals (Figure 8(b), the characteristic peaks at $2\theta = 23.2^{o}$ and 28.0^{o} for Form γ were detected. Also, the DSC scan in Figure 9 exhibited a eutectic behavior for the mixture of SNM crystals and STZ-SNM co-crystals showing a melting point of STZ-SNM co-crystal at 179.8 ^{o}C and another smaller endothermic peak at 156.2 ^{o}C. Also, according to the HPLC data (Figure S11), Inten-II-STZ-SNM co-crystals had the ratio of STZ to SNM of 0.87:1 verifying that the amount of SNM species was more than the one for STZ species, and the excess amount of SNM species was precipitated out as SNM solids along with the 1:1 co-crystal STZ-SNM product. Intensified Method II will need to be optimized in the future.

Solubility, Partition Coefficient and Moisture Stability

The titration method was used to measure the solubility of purchased STZ crystals, purchased SNM crystals, Cocry-STZ-THE co-crystals, Cocry-STZ-SNM

co-crystals, and the blends of purchased STZ and purchased THE crystals, and the blends of purchased STZ and purchased SNM crystals with a molar ratio of 1:1 in water at a variety of temperatures (Figure 10). The solubility values of STZ crystals and STZ-THE co-crystals were not too different from one another (Figure 10(b)). On the other hand, STZ-SNM co-crystals had an obvious increase in the solubility value (Figure 10 (b)). Noticeably, the blends of individual components with STZ crystals exhibited a similar solubility value as the one of STZ crystals, meaning that making a simple drug combo cannot affect the solubility of STZ too much.

Table 3 listed the solubility values of purchased STZ, purchased SNM, Cocry-STZ-THE and Cocry-STZ-SNM co-crystals at a variety of pH values. UV/vis spectrophotometry was employed to measure the solubility value. To confirm the co-crystals were dissolved in water with a 1 to 1 stoichiometric ratio, the suspended solids were filtered and oven dried, and characterized by DSC.

If only the endothermic peak of co-crystal was detected in DSC scan, the ratio of dissolved species of STZ to THE for STZ-THE co-crystals, and the ratio of dissolved species of STZ to SNM for STZ-SNM co-crystals should be equal to 1 to 1. As expected, the DSC scans (not shown) of STZ crystals, SNM crystals and STZ-THE co-crystals exhibited only one melting point meaning that the integrity of the crystal structure was maintained at the pH range of 1 to 8. However, the DSC

scan indicated that STZ crystallized out separately from the solution of STZ-SNM system in an acidic environment. Therefore, the pH solubility values of STZ-SNM co-crystals at low pH could not be measured.

STZ-THE co-crystals exhibited a slightly higher solubility than the one of STZ crystals at the pH range from 3 to 6. The sulfonamide–induced crystalluria frequently occurred during the therapy of sulfonamide, which would cause the kidney lesions.[30] The low solubility of sulfonamide in water is one of the reasons why it deposits in urine, so that the enhancement in its solubility should help to prevent crystalluria formation of sulfonamide.[31] At the pH range from 5.5 to 7, the solubility of STZ-THE co-crystals was higher than the one of STZ crystals. The solubility value of STZ enhanced by co-crystal formation may reduce the likelihood of forming crystalluria of STZ.

Interestingly, the pH-dependent solubility of STZ crystals was altered after co-crystal formation. The solubility value of STZ crystals increased drastically when the pH value was < 2 or >7, and was higher than the solubility value of STZ-THE co-crystals. However, the degree of increase in the solubility value of STZ-THE co-crystals was not as much as the one of STZ crystals. As for STZ-SNM co-crystals, its solubility value was higher than the one of STZ-THE co-crystals but lower than the one of STZ crystals in a basic environment. By taking the advantage

of this property, the degree of separation of the product can be enhanced. Since STZ, SNM, STZ-THE and STZ-SNM species were crystallized out by neutralization, the final pH value was adjusted to 4 or 5 for getting the maximum percent yield of STZ or SNM crystals. However, the final product of Inten-I-STZ-SNM co-crystals was adulterated with a trace of STZ crystals when the final pH was lower to 4 or 5. The endothermic peak of non-co-crystallized STZ solids at around 165.8 ^{o}C was detected by DSC. Since the solubility value of STZ crystals was much higher than the one of STZ-SNM co-crystals when the pH value was > 8, the final pH was raised to 9 for increasing the purity of Inten-I-STZ-SNM co-crystals by allowing the STZ species to remain dissolved in the mother liquor, and only to produce the STZ-SNM co-crystals.

The oil-water partition coefficient, log P, of lornoxicam-saccharin sodium co-crystals had been investigated in the literature.[58] Log P had a significant effect to the absorption, distribution, metabolism and excretion (ADME), and it was determined by the distribution of API molecules in the 1-octanol phase and the aqueous phase. HPLC was used to measure the co-crystal concentration in the aqueous phase. The log P values of STZ-THE and STZ-SNM co-crystals in 1-octanol/water based on the concentration of dissolved STZ species were $-2.1\times10^{-4}\pm0.02$ and $-6.2\times10^{-2}\pm0.06$, respectively, which were lower than 0.05 of STZ species.[59] The log P value of STZ-SNM co-crystals based on the concentration of

dissolved SNM species in 1-octanol/water was -0.93±0.26 which was also lower than -0.62 for SNM species.[59] The decrease in partition coefficient meant that the lipophilicity of STZ and SNM was reduced, but the hydrophilicity was increased.

The Cocry-STZ-THE and Cocry-STZ-SNM co-crystals were stored in a capped glass bottle having an atmosphere of a relative humidity of 75% and a temperature of 40 ^{o}C for a month. The DSC scans of both co-crystals remained the same as shown in Figure S12, indicating that STZ-THE co-crystals, and STZ-SNM co-crystals could be stored in a high relative humidity at 40 ^{o}C for at least a month.

CONCLUSIONS

Co-crystal formation was a potential approach to modify the physicochemical properties of API and to overcome the processing challenges in pharmaceutical industry. 1:1 co-crystal of STZ-THE and 1:1 co-crystal of STZ-SNM were successfully produced by Intensified methods I and II, respectively. The issue of polymorphic impurity for synthesized SNM crystals was solved by co-crystallization. Intensified Method I had reduced the number of processing steps, solvent and energy consumption, and waste generation, and increased the product yields without changing the effective chemical entity, process and facilities substantially. The overall co-crystal percent yields by Intensified Method I were much higher than the

ones by Conventional Method. The purities of the co-crystals achieved by the two methods were almost the same. Co-crystal formation could alter the original thermal behavior of API or co-former, and exhibit eutectic behavior so that the melting points of STZ and SNM crystals were lowered. In the solubility test, the solubility values of STZ-THE co-crystals were close to the ones of STZ crystals, but the solubility values of STZ-SNM co-crystals were higher than the ones of STZ crystals at a variety of temperatures. Co-crystal formation altered the pH-dependent solubility of STZ and SNM crystals. At the pH range from 5.5 to 7, the solubility value of STZ-THE co-crystals was higher than one of STZ crystals. This implied that co-crystal formation improved the solubility of STZ species, and might reduce the possibility of forming crystalluria of STZ species. Besides, it was also applied to dissolve an excessive amount of STZ solids in Inten-I-STZ-SNM co-crystals, so that only pure STZ-SNM co-crystals were achieved when the pH value after neutralization was adjusted to 9. Finally, both STZ-THE and STZ-SNM co-crystals could be stored and remained stable in conditions under 75% relative humidity and at 40^{o}C for at least one month. In our future work, process analytical technology (PAT) may be used to monitor nucleation and crystal growth occurring in this system. We hope that the present intensified processes can be applied in many other systems and extended to solvent-less production processes for co-crystals.

ASSOCIATED CONTENT

Supporting Information

The Supporting Information is available free of charge on the ACS Publications website at DOI:

FT-IR spectra, TGA and DSC scans, PXRD patterns, ^{1}H-NMR spectra, HPLC chromatograms and equations for the curve fittings of the solubility

ACKNOWLEDGEMENT

This research was supported by the grants from the Ministry of Science and Technology of Taiwan R.O.C. (MOST 104-2221-E-008 -070-MY3). We are greatly indebted to Mrs. Jui-Mei Huang for the assistance in DSC and TGA at the Precision Instrument Center and Ms. Hsiu-Luan Chen for the help in NMR at Instrumentation Center of National Central University, and Mr. Tzu-Chiang Lu for the assistance in HPLC at the Chunghwa Chemical Synthesis & Biotech Co., Ltd.

For Table of Contents Use Only

Intensified Crystallization Processes for 1:1 Drug-Drug Co-crystals of Sulfathiazole-Theophylline, and Sulfathiazole-Sulfanilamide

Kuan Lin Yeh and Tu Lee*

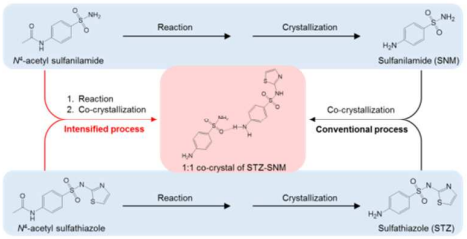

In the Conventional Method, 1:1 co-crystal of sulfathiazole-sulfanilamide was produced by co-crystallization of the two drugs, which was individually synthesized. In the Intensified Method, chemical synthesis and co-crystallization were integrated to give the co-crystals. The number of processing steps was reduced, and the percent yield of co-crystals was enhanced with high purity.

REFERENCES

[1] Thakuria, R.; Delori, A.; Jones, W.; Lipert, M. P.; Roy, L.; Rodríguez-Hornedo, N. Pharmaceutical Cocrystals and Poorly Soluble Drugs. *Int. J. Pharm*. **2013**, *453*, 101-125.

[2] Schultheiss, N.; Newman, A. Pharmaceutical Cocrystals and Their Physicochemical Properties. *Cryst. Growth Des.* **2009**, *9*, 2950-2967.

[3] Sarcevica, I.; Orola, L.; Veidis, M. V.; Podjava, A.; Belyakov, S. Crystal and Molecular Structure and Stability of Isoniazid Cocrystals with Selected Carboxylic Acids. *Cryst. Growth Des*. **2013**, *13*, 1082-1090.

[4] Lu, J.; Rohani, S. Preparation and Characterization of Theophylline-Nicotinamide Cocrystal. *Org. Process Res. Dev*. **2009**, *13*, 1269-1275.

[5] Qiao, N.; Li, M.; Schlindwein, W.; Malek, N.; Davies, A.; Trappitt, G. Pharmaceutical Cocrystals: An Overview. *Int. J. Pharm.* **2011**, *419*, 1-11.

[6] Sanphui, P.; Mishra, M. K.; Ramamurty, U.; Desiraju, G. R. Tuning Mechanical Properties of Pharmaceutical Crystals with Multicomponent Crystals: Voriconazole as a Case Study. *Mol. Pharmaceutics* **2015**, *12*, 889-897.

[7] Lee, T.; Chen, J. W.; Lee, H. L.; Lin, T. Y.; Tsai, Y. C.; Cheng, S.-L.; Lee, S.-W.; Hu, J.-C.; Chen, L.-T. Stabilization and Spheroidization of Ammonium Nitrate: Co-Crystallization with Crown Ethers and Spherical Crystallization by Solvent

Screening. *Chem. Eng. J*. **2013**, *225*, 809-817.

[8] Censi, R.; Di Martino, P. Polymorph Impact on the Bioavailability and Stability of Poorly Soluble Drugs. *Molecules* **2015**, *20*, 18759-18776.

[9] Duggirala, N. K.; Perry, M. L.; Almarsson, Ö.; Zaworotko, M. J. Pharmaceutical Cocrystals: Along the Path to Improved Medicines. *Chem. Commun*. **2016**, *52*, 640-655.

[10] Almarsson, Ö.; Vadas, E. B. Molecules, Materials, Medicines (M3): Linking Molecules to Medicines through Pharmaceutical Material Science. *Cryst. Growth Des*. **2015**, *15*, 5645-5647.

[11] Wang, H.; Mustaffar, A.; Phan, A. N.; Zivkovic, V; Reay, D.; Law, R.; Boodhoo, K. A Review of Process Intensification Applied to Solids Handling. *Chem. Eng. Process.* **2017**, *118*, 78-107.

[12] Stankiewicz, A. I.; Moulijn, J. A. Process Intensification: Transforming Chemical Engineering. *Chem. Eng. Prog*. **2000**, *96*, 22-34.

[13] Lee, T.; Lin, H. Y.; Lee, H. L. Engineering Reaction and Crystallization and the Impact on Filtration, Drying, and Dissolution Behaviors: The Study of Acetaminophen (Paracetamol) by In-Process Controls. *Org. Process Res*. *Dev*. **2013**, *17*, 1168-1178.

[14] Ståhl, M.; Åslund, B. L.; Rasmuson, Å. C. Reaction Crystallization Kinetics of

Benzoic Acid. *AlChE J*. **2001**, *47*, 1544-1560.

[15] Lee, H. L.; Lee, T. Direct Co-crystal Assembly from Synthesis to Co-crystallization. *CrystEngComm* **2015**, *17*, 9002-9006.

[16] Caira, M. R. Sulfa Drugs as Model Cocrystal Formers. *Mol. Pharmaceutics* **2007**, *4*, 310-316.

[17] Becheker, I.; Berredjem, H.; Boutefnouchet, N.; Berredjem, M.; Ladjama, A. Antibacterial Activity of Four Sulfonamide Derivatives against Multidrug-Resistant Staphylococcus Aureus. *J. Chem. Pharm. Res.* **2014**, *6*, 893-899.

[18] Park, S.-J.; Yeo, S.-D. Antisolvent Crystallization of Sulfa Drugs and the Effect of Process Parameters. *Sep. Sci. Technol*. **2007**, *42*, 2645-2660.

[19] Hu, Y.; Gniado, K.; Erxleben, A.; McArdle, P. Mechanochemical Reaction of Sulfathiazole with Carboxylic Acids: Formation of a Cocrystal, a Salt, and Coamorphous Solids. *Cryst. Growth De*s. **2014**, *14*, 803-813.

[20] Shefter, E.; Sackman, P. Structural Studies on Molecular Complexes V: Crystal Structures of Sulfathiazole-Sulfanilamide and Sulfathiazole-Theophylline Complexes. *J. Pharm. Sci*. **1971**, *60*, 282-286.

[21] Samanta, R.; Kanaujia, S.; Reddy, C. M. New Co-crystal and Salt Form of Sulfathiazole with Carboxylic Acid and Amide. *J. Chem. Sci*. **2014**, *126*, 1363-1367.

[22] Suresh, K.; Minkov, V. S.; Namila, K. K.; Derevyannikova, E.; Losev, E.; Nangia,

A.; Boldyreva, E. V. Novel Synthons in Sulfamethizole Cocrystals: Structure–Property Relations and Solubility. *Cryst. Growth Des*. **2015**, *15*, 3498-3510.

[23] Aitipamula, S.; Chow, P. S.; Tan, R. B. H. Trimorphs of a Pharmaceutical Cocrystal Involving Two Active Pharmaceutical Ingredients: Potential Relevance to Combination Drugs. *CrystEngComm* **2009**, *11*, 1823-1827.

[24] Chou, T.-C. Drug Combination Studies and Their Synergy Quantification Using the Chou-Talalay Method. *Cancer Res*. **2010**, *70*, 440-446.

[25] Chou, T. C. Theoretical Basis, Experimental Design, and Computerized Simulation of Synergism and Antagonism in Drug Combination Studies. *Pharmacol. Rev*. **2006**, *58*, 621-681.

[26] Thipparaboina, R.; Kumar, D; Chavan, R. B.; Shastri, N. R. Multidrug Co-crystals: Towards the Development of Effective Therapeutic Hybrids. *Drug Discovery Today* **2016**, *21*, 481-490.

[27] Fischbach, M. A. Combination Therapies for Combating Antimicrobial Resistance. *Curr. Opin. Microbiol.* **2011**, *14*, 519-523.

[28] Feng, L.; Karpinski, P. H.; Sutton, P.; Liu, Y.; Hook, D. F.; Hu, B.; Blacklock, T. J.; Fanwick, P. E.; Prashad, M.; Godtfredsen, S.; Ziltener, C. LCZ696: A Dual-Acting Sodium Supramolecular Complex. *Tetrahedron Lett.* **2012**, *53*, 275-276.

[29] Grobelny, P.; Mukherjee, A.; Desiraju, G. R. Drug-Drug Co-crystals:

Temperature-Dependent Proton Mobility in the Molecular Complex of Isoniazid with 4-Aminosalicylic Acid. *CrystEngComm* **2011**, *13*, 4358-4364.

[30] Lehr, D.; Slobody, L.; Greenberg, W. The Use of a Sulfadiazine-Sulfathiazole Mixture in the Treatment of Children. *J. Pediatr.* **1946**, *29*, 275-285.

[31] Schwartz, L.; Flippin, H. F.; Reinhold, J. G.; Domm, A. H. The Effect of Alkali on Crystalluria from Sulfathiazole and Sulfadiazine. *JAMA, J. Am. Med. Assoc.* **1941**, *117*, 514-515.

[32] Lee, T.; Chen, Y. H.; Zhang, C. W. Solubility, Polymorphism, Crystallinity, Crystal Habit, and Drying Scheme of (*R,S*)-(±)-Sodium Ibuprofen Dihydrate. *Pharm. Technol*. **2007**, *31*, 72-87.

[33] Bakar, M. R. A.; Nagy, Z. K.; Rielly, C. D.; Dann, S. E. Investigation of the Riddle of Sulfathiazole Polymorphism. *Int. J. Pharm*. **2011**, *414*, 86-103.

[34] Ildiz, G. O.; Akyuz, S. Conformational Analysis and Vibrational Study of Sulfanilamide. *Vib. Spectrosc*. **2012**, *58*, 12-18.

[35] Ehiwe, T. O.; Alexander, B. D.; Mitchell, J. C.; Snowden, M. J.; Waters, L. J. Monitoring Real Time Polymorphic Transformation of Sulfanilamide by Diffuse Reflectance Visible Spectroscopy. *J. Pharm. Anal*. **2016**, *6*, 179-183.

[36] Munroe, Á.; Rasmuson, Å. C.; Hodnett, B. K.; Croker, D. M. Relative Stabilities of the Five Polymorphs of Sulfathiazole. *Cryst. Growth Des.* **2012**, *12*, 2825-2835.

[37] Portieri, A.; Harris, R. K.; Fletton, R. A.; Lancaster, R. W.; Threlfall, T. L. Effects of Polymorphic Differences for Sulfanilamide, as Seen through ^{13}C and ^{15}N Solid-State NMR, Together with Shielding Calculations. *Magn. Reson. Chem*. **2004**. *42*, 313-320.

[38] Apperley, D. C.; Fletton, R. A.; Harris, R. K.; Lancaster, R. W.; Tavener, S.; Threlfall, T. L. Sulfathiazole Polymorphism Studied by Magic-Angle Spinning NMR. *J. Pharm. Sci.* **1999**, *88*, 1275-1280.

[39] Lin, H. O.; Guillory, J. K. Polymorphism in Sulfanilamide-d_4. *J. Pharm, Sci*. **1970**, *59*, 972-975.

[40] Cleary Jr., T. F. Process for Preparing Sulfathiazole. U. S. Patent 2,592,860, April 15, 1952.

[41] Boyle, J; Otty, S.; Sarojini, V. A Safer and Convenient Synthesis of Sulfathiazole for Undergraduate Organic and Medicinal Chemistry Classes. *J. Chem. Educ.* **2012,** *89*, 141-143.

[42] Bellú, S.; Hure, E.; Trapé, M.; Rizzotto, M.; Sutich, E.; Sigrist, M.; Moreno, V. The Interaction between Mercury (II) and Sulfathiazole. *Quim. Nova* **2003**, *26*, 188-192.

[43] Anderson, J. E.; Moore, S.; Tarczynski, F.; Walker, D. Determination of the Onset of Crystallization of N^1-2-(Thiazolyl)Sulfanilamide (Sulfathiazole) by UV-Vis and Calorimetry Using an Automated Reaction Platform; Subsequent Characterization of

Polymorphic Forms Using Dispersive Raman Spectroscopy. *Spectrochim. Acta, Part A* **2001**, *57*, 1793-1808.

[44] Varghese, H. T.; Panicker, C. Y.; Anto, P. L; Philip, D. Potential Dependent SERS Profile of Sulfanilamide on Silver Electrode. *J. Raman Spectrosc.* **2006**, *37*, 487-491.

[45] Cullity, B. D.; Stock, S. R. Diffraction III: Real Samples. *Elements of X-ray Diffraction*, 3rd Edition; Pearsons Eduction Limited: London, 2001; pp 174-177.

[46] Ostwald, W. Studien über die Bildung und Umwandlung fester Körper. *Z. Phys. Chem.* **1897**, *22*, 289-330.

[47] Chemburkar, S. R.; Bauer, J.; Deming, K.; Spiwek, H.; Patel, K.; Morris, J.; Henry, R.; Spanton, S.; Dziki, W.; Porter, W.; Quick, J.; Bauer, P.; Donaubauer, J.; Narayanan, B. A.; Soldani, M.; Riley, D.; McFarland, K. Dealing with the Impact of Ritonavir Polymorphs on the Late Stages of Bulk Drug Process Development. *Org. Process Res. Dev.* **2000**, *4*, 413-417.

[48] Xu, D.; Xue, D. Chemical Bond Analysis of the Crystal Growth of KDP and ADP. *J. Cryst. Growth* **2006**, *286*, 108-113.

[49] Haines, P. J. Differential Thermal Analysis and Differential Scanning Calorimetry. *Thermal Methods of Analysis: Principles*, *Applications and Problems*; Blackie Academic & Professional: New York, 1995; pp 89.

[50] Li, Z. J.; Ojala, W. H.; Grant, D. J. W. Molecular Modeling Study of Chiral Drug

Crystals: Lattice Energy Calculations. *J. Pharm. Sci*. **2001**, *90*, 1523-1539.

[51] McNamara, D. P; Childs, S. L.; Giordano, J.; Iarriccio, A.; Cassidy, J.; Shet, M. S.; Mannion, R.; O'Donnell, E.; Park, A. Use of a Glutaric Acid Cocrystal to Improve Oral Bioavailability of a Low Solubility API. *Pharm. Res.* **2006**, *23*, 1888-1897.

[52] Cherukuvada, S.; Guru Row, T. N. G. Comprehending the Formation of Eutectics and Cocrystals in Terms of Design and Their Structural Interrelationships. *Cryst. Growth Des.* **2014**, *14*, 4187-4198.

[53] Cherukuvada, S.; Nangia, A. Fast Dissolving Eutectic Compositions of Two Anti-tubercular Drugs. *CrystEngComm* **2012**, *14*, 2579-2588.

[54] Padrela, L.; de Azevedo, E. G.; Velaga, S. P. Powder X-ray Diffraction Method for the Quantification of Cocrystals in the Crystallization Mixture. *Drug Dev. Ind. Pharm.* **2012**, *38*, 923-929.

[55] Spectral Database for Organic Compounds SDBS http://sdbs.db.aist.go.jp (National Institute of Advanced Industrial Science and Technology, last assessed on August 17)

[56] Garekani, H. A.; Sadeghi, F.; Badiee, A.; Mostafa, S. A.; Rajabi-Siahboomi, A. R. Crystal Habit Modifications of Ibuprofen and Their Physicomechanical Characteristics. *Drug Dev. Ind. Pharm*. **2001**, *27*, 803-809.

[57] Tung, H.-H,; Paul, E. L.; Midler, M.; McCauley, J. A. Properties. *Crystallization of Organic Compounds, An Industrial Perspective*; A John Wiley & Sons, Inc: New York,

2009; pp 44.

[58] Gadade, D. D.; Kulkarni, D. A.; Rathi, P. B.; Pekamwar. S. S.; Joshi, S. S. Solubility Enhancement of Lornoxicam by Crystal Engineering. *Indian J. Pharm. Sci.* **2017**, *79*, 277-286.

[59] Pyka, A.; Babuśka, M.; Zachariasz, M. A Comparison of Theoretical Methods of Calculation of Partition Coefficients for Selected Drugs. *Acta Pol. Pharm*. **2006**, *63*, 159-167.

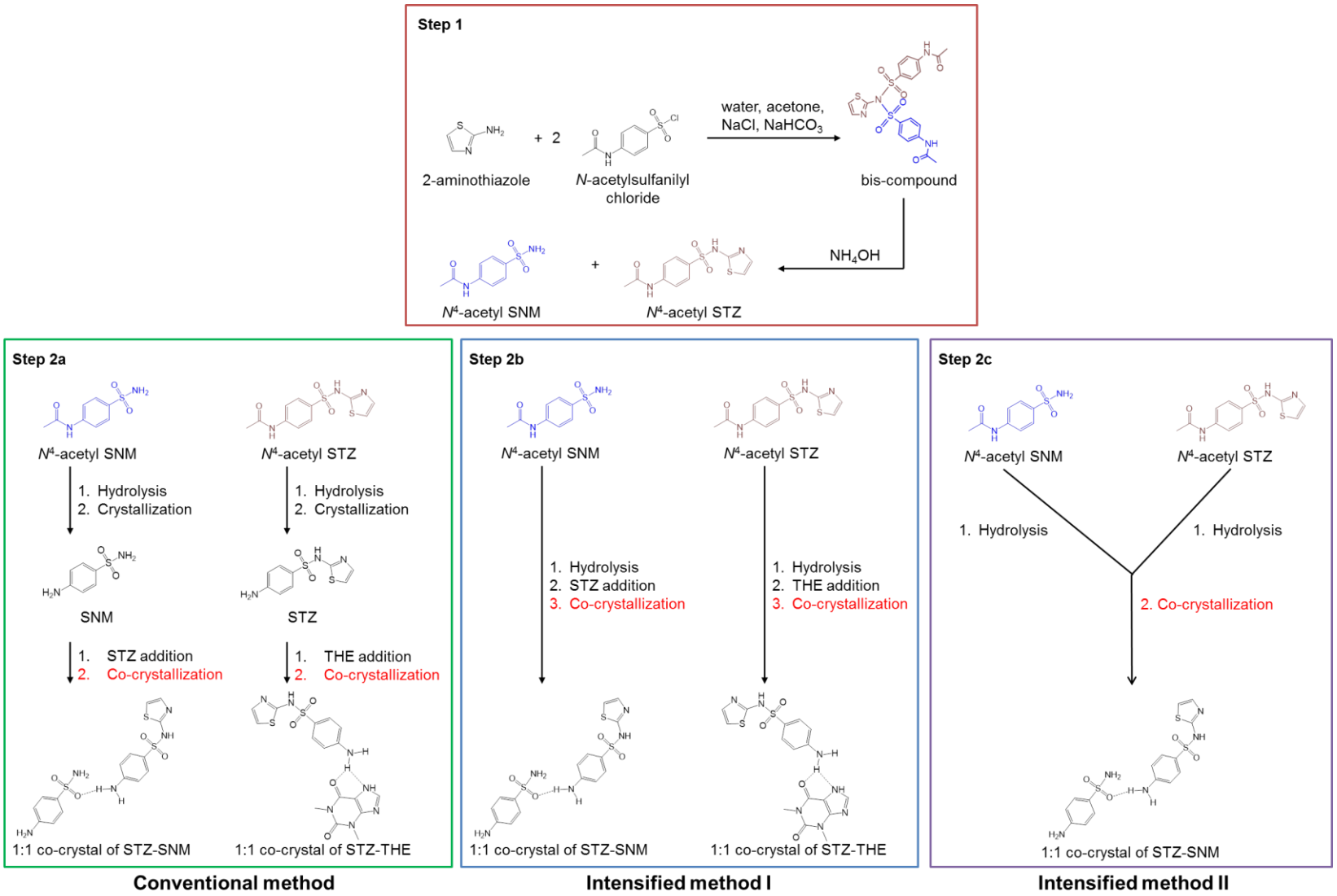

Scheme 1. Processes of Conventional Method, Intensified Methods I and II.

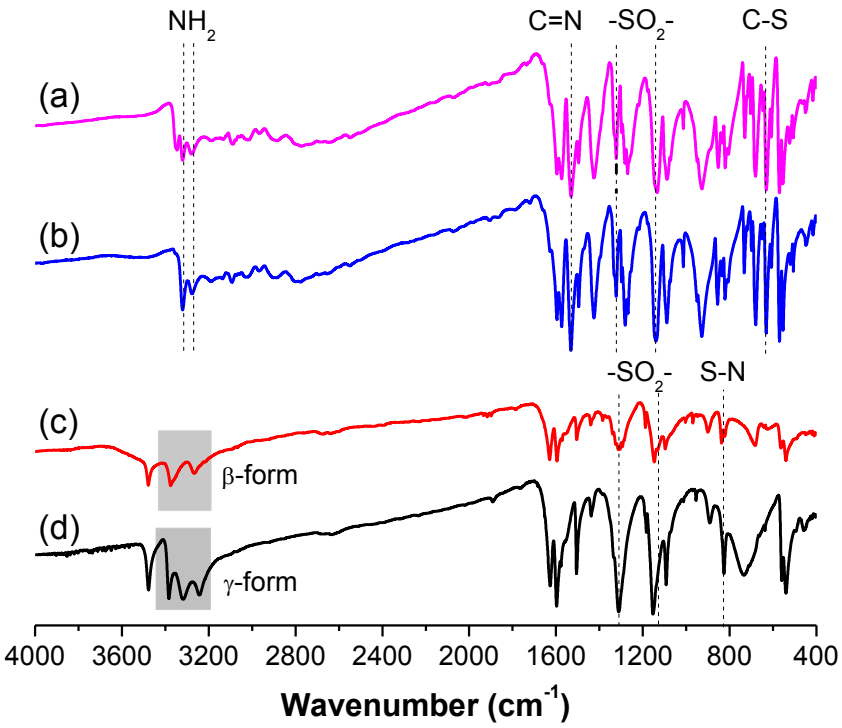

Figure 1. FT-IR spectra of (a) purchased STZ crystals, (b) synthesized STZ crystals, (c) purchased SNM crystals, and (d) synthesized SNM crystals.

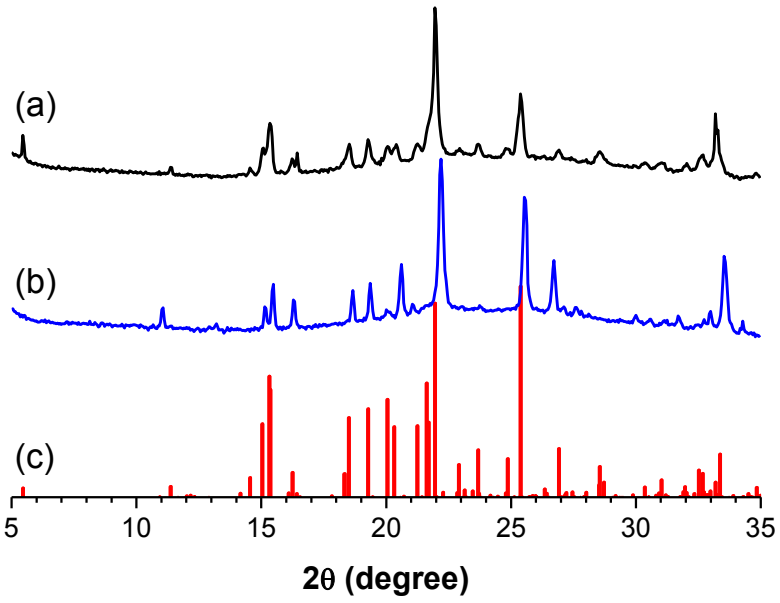

Figure 2. PXRD patterns of (a) purchased STZ crystals, (b) synthesized STZ crystals, and (c) theoretical diffraction pattern of Form III STZ crystals (CCDC code: SUTHZ02).

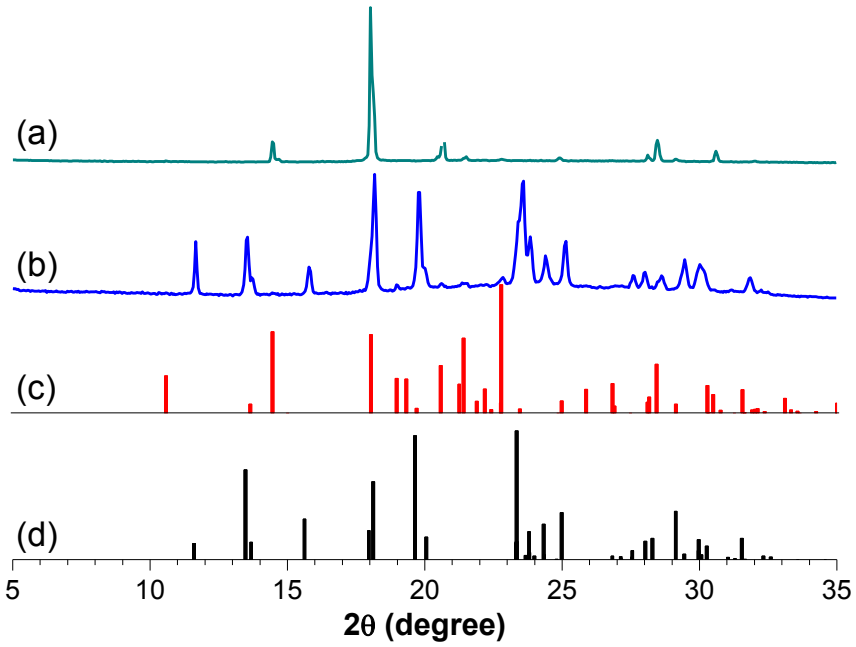

Figure 3. PXRD patterns of (a) purchased SNM crystals, (b) synthesized SNM crystals, (c) theoretical diffraction pattern of Form β SNM crystals (SULAMD03), and (d) theoretical diffraction pattern of Form γ SNM crystals (CCDC code: SULAMD02).

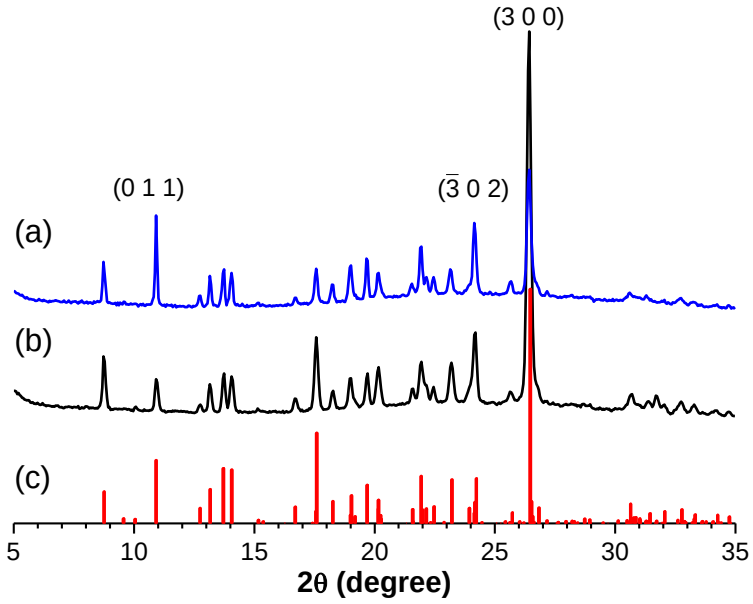

Figure 4. PXRD patterns of (a) Cocry-STZ-THE co-crystals, (b) Inten-I-STZ-THE co-crystals, and theoretical diffraction pattern of STZ-THE co-crystals (CCDC code: SULTHE01).

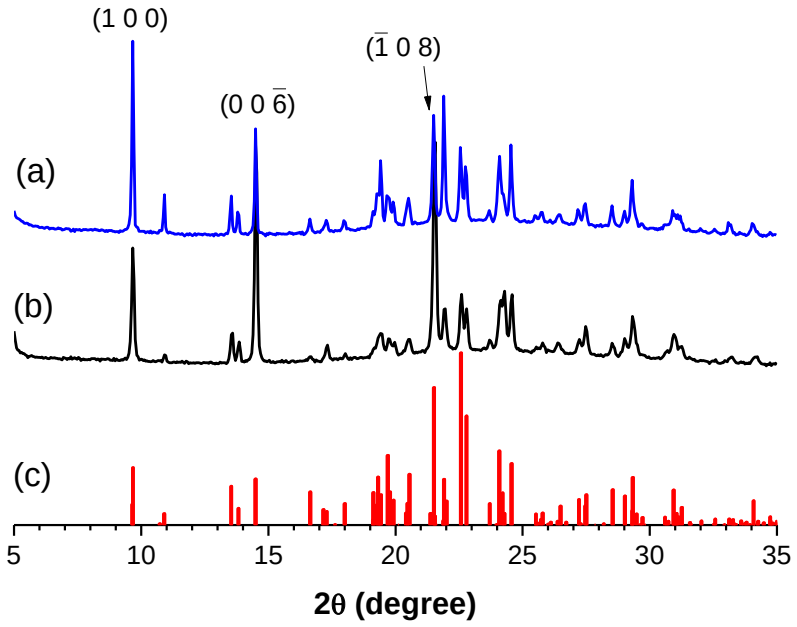

Figure 5. PXRD patterns of (a) Cocry-STZ-SNM co-crystals, (b) Inten-I-STZ-SNM co-crystals, and (c) theoretical diffraction pattern of STZ-SNM co-crystals (CCDC code: STHSAM01).

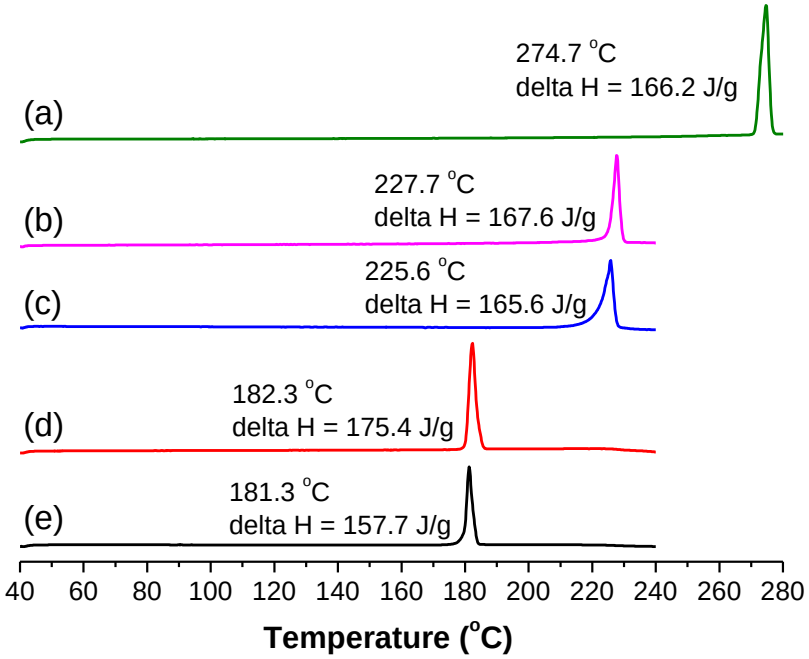

Figure 6. DSC scans of (a) purchased THE crystals, (b) Cocry-STZ-THE co-crystals, (c) Inten-I-STZ-THE co-crystals, (d) Cocry-STZ-SNM co-crystals, and (e) Inten-I-STZ-SNM co-crystals.

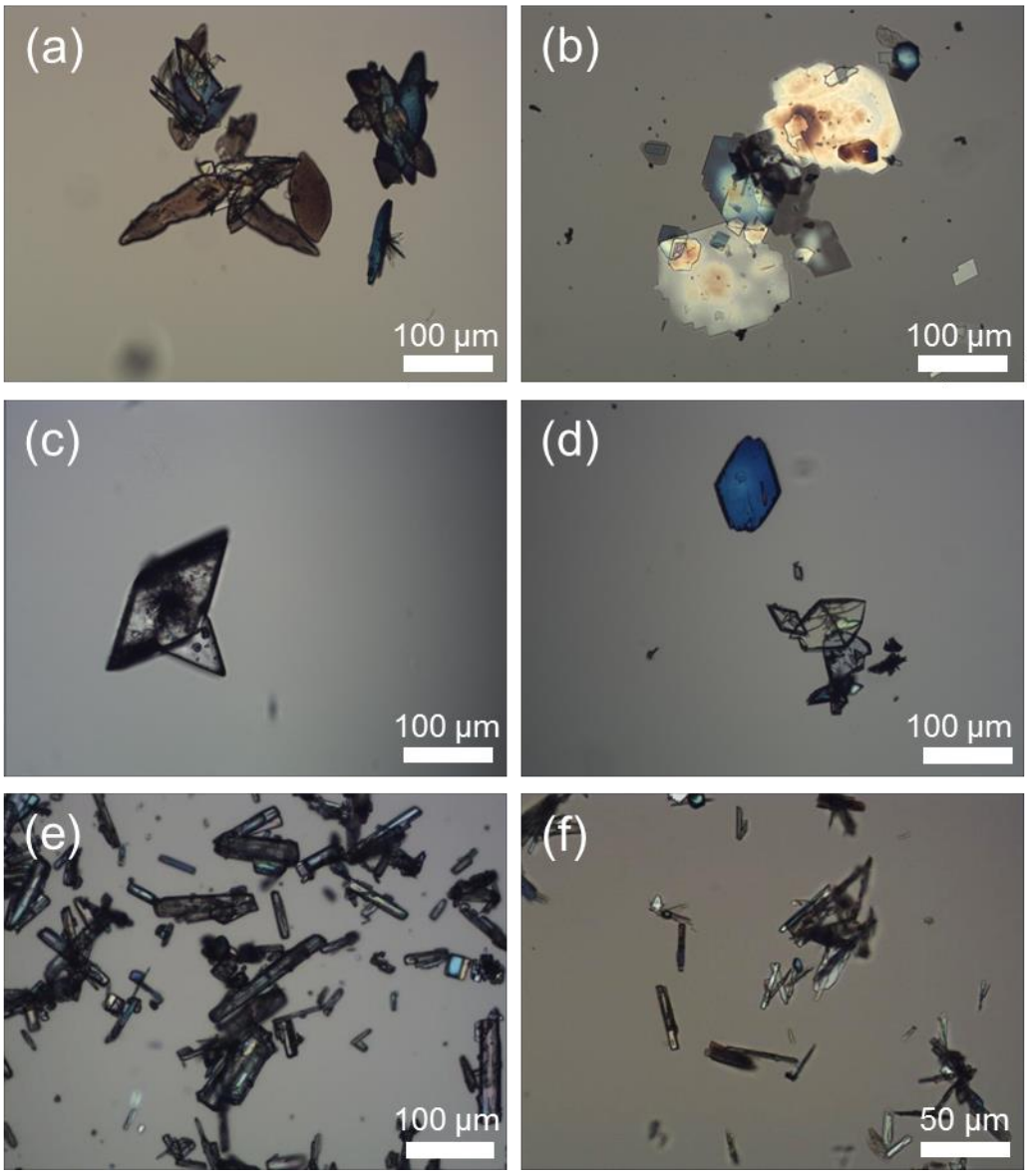

Figure 7. OM images of (a) synthesized STZ crystals, (b) synthesized SNM crystals, (c) Cocry-STZ-THE co-crystals, (d) Inten-I-STZ-THE co-crystals, (e) Cocry-STZ-SNM co-crystals, and (f) Inten-I-STZ-SNM co-crystals.

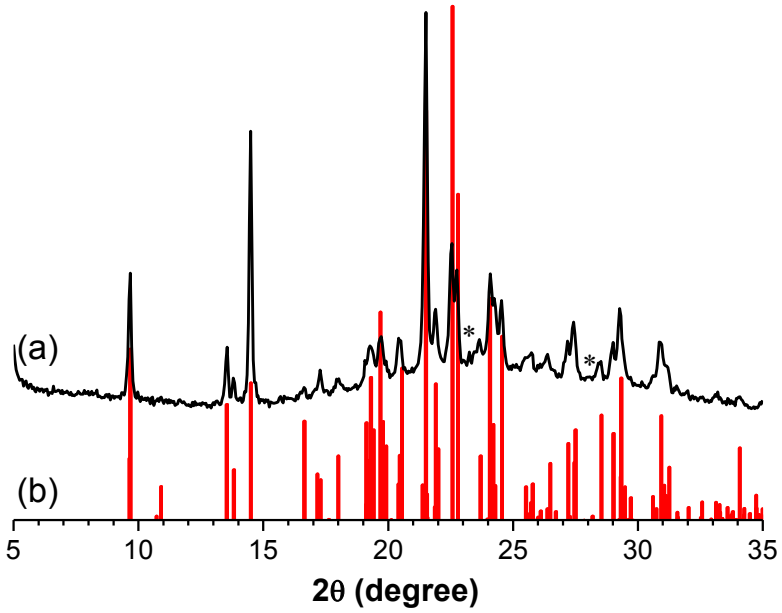

Figure 8. PXRD diffraction patterns of (a) Inten-II-STZ-SNM co-crystals, and (b) theoretical diffraction pattern of STZ-SNM co-crystals (*: diffraction peaks of Form γ SNM).

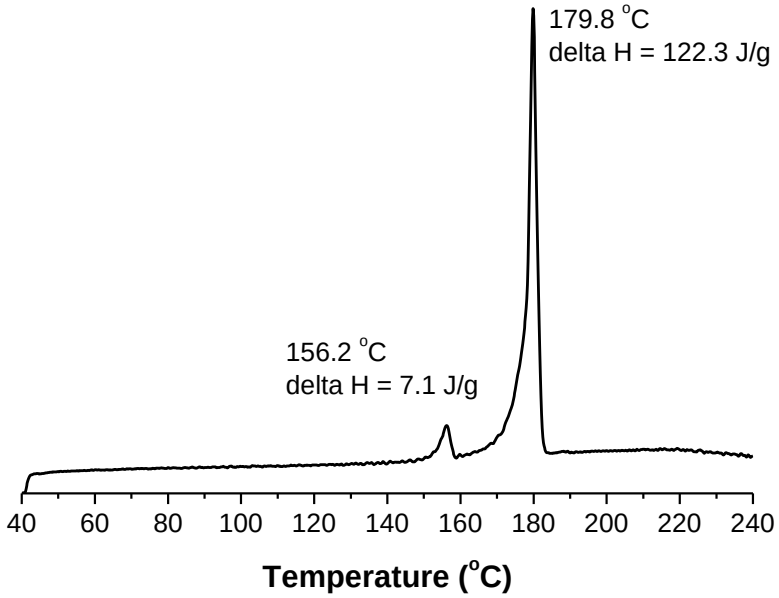

Figure 9. DSC scan of Inten-II-STZ-SNM co-crystals.

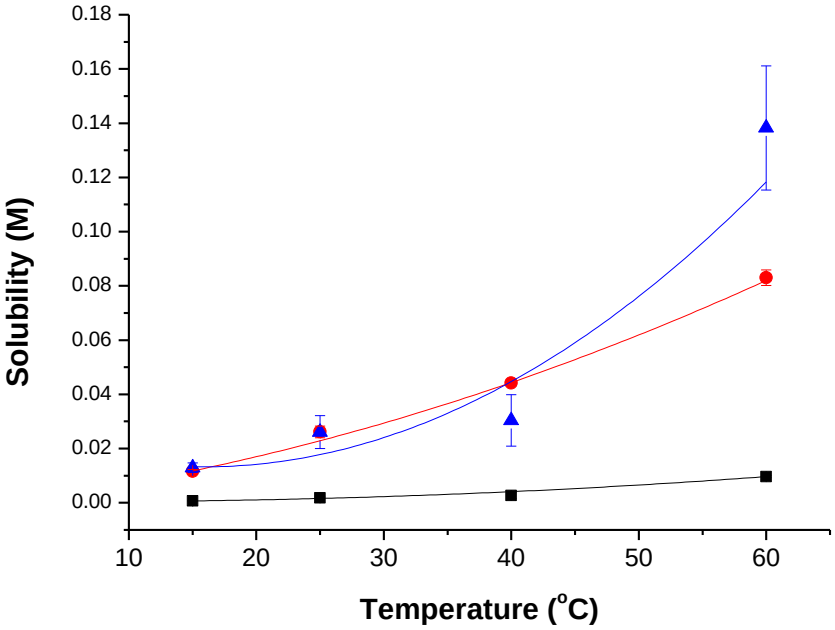

(a)

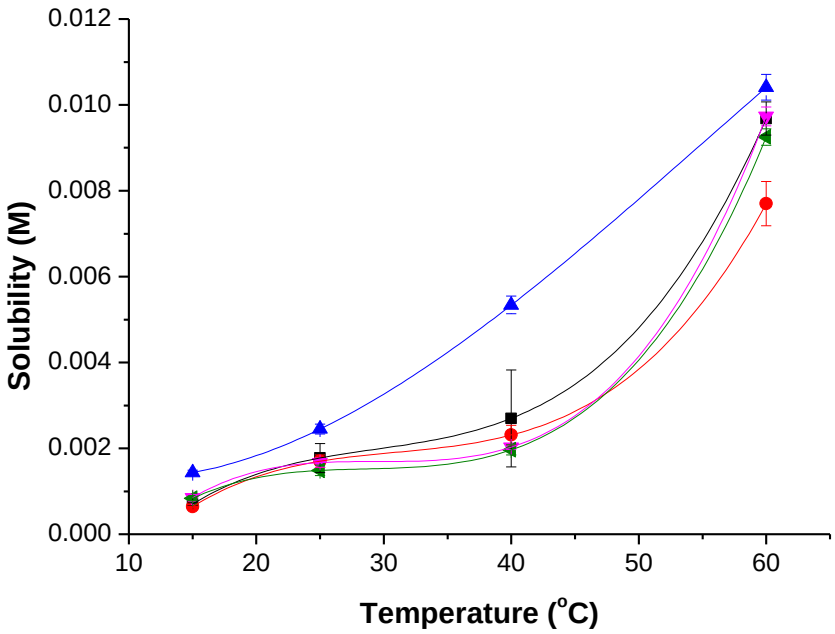

(b)

Figure 10. Solubility curves of (a) ■ purchased STZ crystals, ● purchased SNM crystals, ▲purchased THE crystals, (b) ■ purchased STZ crystals , ● Cocry-STZ-THE co-crystals , ▲ Cocry-STZ-SNM co-crystals, ▼ physical blend of purchased STZ and purchased THE crystals with a molar ratio of 1:1 in water, and ◀ physical blend of purchased STZ and purchased SNM crystals with a molar ratio of 1:1 in water.

Table 1. The comparison of the product yields from different methods.

Method / Sample	STZ-THE		STZ-SNM	
	Conventional (%)	Intensified (%)	Conventional (%)	Intensified (%)
Synthesized STZ	60.6			
Synthesized SNM			52.4	
Cocry-STZ-THE	68.1			
Cocry-STZ-SNM			73.8	
Inten-I-STZ-THE		81.0		
Inten-I-STZ-SNM				73.7
Overall	41.3	81.0	38.7	73.7

The yields were calculated as the experiment weight of product divided by the theoretical weight of products multiplied by 100%.

Table 2. HPLC results of the crystals harvested from different methods.

Sample	Purity (%)	Component Ratio	Retention Time (min)
Synthesized STZ	99.2		6.4
Synthesized SNM	99.5		3.3
Inten-I-STZ-THE	99.0	1.03:1 (STZ:THE)	6.4 (STZ) / 7.2 (THE)
Inten-I-STZ-SNM	99.4	1.06:1 (STZ:SNM)	3.4 (SNM) / 6.5 (STZ)
Inten-II-STZ-SNM	98.3	0.87:1 (STZ:SNM)	3.3 (SNM) / 6.4 (STZ)

Table 3. Solubility values of purchased STZ crystals, purchased SNM crystals, Cocry-STZ-THE co-crystals and Cocry-STZ-SNM co-crystals at various pH values and 37 ^{o}C in water.

Sample	pH	Solubility (10^3 M)
Purchased STZ	1.15	35.63
	1.67	9.12
	2.52	4.18
	3.36	3.08
	4.95	2.67
	5.19	2.77
	5.67	3.06
	6.80	4.07
	7.47	8.51
	8.20	37.56
Purchased SNM	1.53	97.96
	2.65	94.09
	3.71	77.83
	4.51	67.68
	6.22	66.10
	6.85	71.73
	7.41	75.25
	8.27	79.73
Cocry-STZ-THE	1.07	14.55
	1.54	7.92
	2.34	3.95
	3.44	3.28
	4.87	3.39
	5.62	3.26
	6.39	3.77
	7.15	4.42
	7.81	7.67
	8.20	14.11
Cocry-STZ-SNM	7.29	7.29
	7.96	15.01
	8.19	19.43